

Thermal conductivity of $R\text{Ni}_2\text{B}_2\text{C}$ ($R=\text{Y}, \text{Ho}$) single crystals

M. Sera, S. Kobayash, M. Hiroi, and N. Kobayashi

Institute for Materials Research, Tohoku University, Sendai 980, Japan

H. Takeya

National Institute for Metals, 1-2-1, Sengen, Tsukuba, Ibaraki 305, Japan

K. Kadowaki

Institute of Materials Science, University of Tsukuba, Ibaraki 305, Japan

(Received 19 March 1996)

We have studied the thermal conductivity κ of high-quality single crystals of $\text{YNi}_2\text{B}_2\text{C}$ and $\text{HoNi}_2\text{B}_2\text{C}$. In both compounds, κ in the normal state at low temperatures is dominated by electrons. In $\text{YNi}_2\text{B}_2\text{C}$, κ shows a pronounced enhancement around 4 K well below the superconducting transition temperature $T_c = 15.6$ K. It may be due to the increase of the phonon contribution below T_c as a result of the decrease of the number of normal electrons as scattering centers of phonons. This enhancement is suppressed largely by applying the magnetic field of H_{c1} because phonons are scattered by vortices. In $\text{HoNi}_2\text{B}_2\text{C}$, κ shows a discontinuous increase at the Néel temperature $T_N = 4.6$ K and a clear decrease below $T_c \sim 3.6$ K. [S0163-1829(96)03130-X]

Since the recent discovery of the superconductivity in $R\text{Ni}_2\text{B}_2\text{C}$ ($R=\text{Y}, \text{Ho}$, etc.) (Refs. 1,2), extensive studies have been performed in the related compounds which have relatively high superconducting transition temperature T_c . Their crystal structure is of the layered type and they have attracted much attention in relation to high- T_c cuprates. However, the band calculation indicates that the electronic structure is three dimensional and many experimental results suggest that these materials are the conventional phonon mediated s -wave superconductor.^{3,4} However, these materials also exhibit unexpected behavior from an s -wave superconductor. For example, in $\text{YNi}_2\text{B}_2\text{C}$ and $\text{LuNi}_2\text{B}_2\text{C}$, the coherent peak in the NMR relaxation rate below T_c has not been observed (Ref. 5) and the specific heat shows $\sim T^3$ behavior in a wide range of temperature below T_c .^{6,7} Further studies are necessary to clarify the mechanism of the superconductivity in the present system. The thermal conductivity κ is very useful to investigate the nature of the superconducting state and has been studied extensively on heavy Fermion superconductors and high- T_c cuprates in recent years. In high- T_c cuprates, it is well known that the pronounced enhancement of κ is observed below T_c and the recent results under the magnetic field indicate that its origin is the huge enhancement of the lifetime of quasiparticles below T_c .⁸ In a conventional low- T_c s -wave superconductor, the phonon contribution to κ increases below T_c due to the decrease of the number of normal electrons as scattering centers of phonons and the electron contribution decreases rapidly below T_c . Whether the observed thermal conductivity increases or decreases below T_c depends on which contribution of phonons and electrons is dominant.

The thermal conductivity of $R\text{Ni}_2\text{B}_2\text{C}$ has not yet been reported. In order to get information on the electron-phonon interaction and the low-energy excitation in the superconducting state in the present system, the thermal conductivities of high-quality single crystals of $\text{YNi}_2\text{B}_2\text{C}$ samples 1 and 2 and $\text{HoNi}_2\text{B}_2\text{C}$ were measured. All the samples used in the

present experiments are single crystals grown by the floating-zone method which is described elsewhere.⁹ The samples were in the form of a parallelepiped with dimensions $0.7 \times 0.7 \times 4 \sim 7$ mm³. The thermal conductivity κ was measured by the usual steady-state method. The temperature gradient of both ends of the samples in the zero magnetic field at high temperatures and under the magnetic field was measured by the AuFe-Chromel thermocouple and two Cernox thermometers, respectively. The electrical resistivity ρ was measured by the usual four-probe method. The error bar of the absolute value of κ and ρ is about 10–15 % and 20–30 %, respectively, depending on the sample size. The residual resistivity of $\text{YNi}_2\text{B}_2\text{C}$ samples 1 and 2 and $\text{HoNi}_2\text{B}_2\text{C}$ are ~ 2.0 , 4.1 , and 3.1 $\mu\Omega$ cm, respectively. The de Haas–van Alphen effect was observed in the samples of $\text{YNi}_2\text{B}_2\text{C}$ sample 1 cut from the same ingot.¹⁰ The magnetostriction was measured by the three terminal capacitance method.¹¹ The specific heat was measured by the usual adiabatic heat pulse method for the same $\text{HoNi}_2\text{B}_2\text{C}$ crystals as those used in the κ and ρ with a weight of 56 mg.

Figure 1 shows the temperature dependence of the thermal conductivity κ of $\text{YNi}_2\text{B}_2\text{C}$ sample 1. The inset shows the temperature dependence of the reduced Lorenz number L/L_0 of the same sample which was derived from the observed κ and ρ . Here, $L_0 = 24.5$ nW Ω K⁻² is the Sommerfeld value and $L = \kappa\rho/T$. Along the a axis, L/L_0 is nearly 1 at low temperatures below ~ 20 K in the normal state. The absolute values of κ of $\text{YNi}_2\text{B}_2\text{C}$ sample 2 at $T = 20$ K are 110 and 103 mW/K cm along the a and c axes, respectively. The difference of the absolute value of κ at low temperatures between samples 1 and 2 by a factor of two is almost the same as that of the residual resistivities between these samples. These results indicate that in the normal state at low temperatures, κ is limited by the impurity scattering, i.e., the elastic scattering of electrons by impurities is dominant and heat current is carried mainly by electrons. Rough estimation of the electronic thermal conductivity κ_e at low temperature

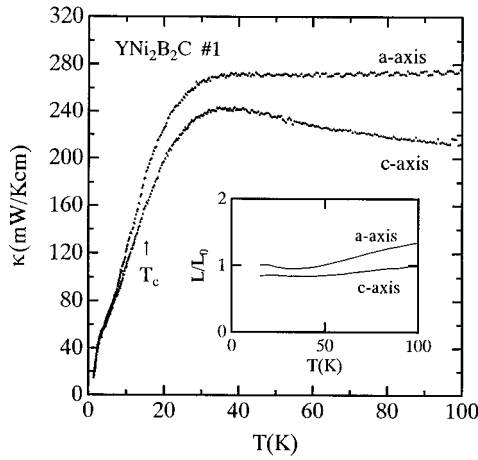


FIG. 1. Temperature dependence of the thermal conductivity with heat current J parallel to the a and c axes of $\text{YNi}_2\text{B}_2\text{C}$, sample 1. The inset shows the temperature dependence of the reduced Lorenz number L/L_0 of sample 1. See the text in detail.

by using the results of the electronic specific heat (Ref. 6) and the electrical resistivity is consistent with the observed result. κ shows a small but clear decrease at $T_c = 15.6$ K and a pronounced enhancement around 4 K which is clearly seen in an expanded scale in Fig. 2. This characteristic behavior is observed also in sample 2 with twice larger residual resistivity. At high temperatures above ~ 40 K, κ shows the anisotropic behavior, i.e., κ with heat current J parallel to the a axis is larger than that parallel to the c axis. This anisotropic behavior of κ at high temperatures is common to $\text{YNi}_2\text{B}_2\text{C}$ samples 1 and 2 and $\text{HoNi}_2\text{B}_2\text{C}$, while their electrical resistivities are almost isotropic. κ parallel to the c axis of

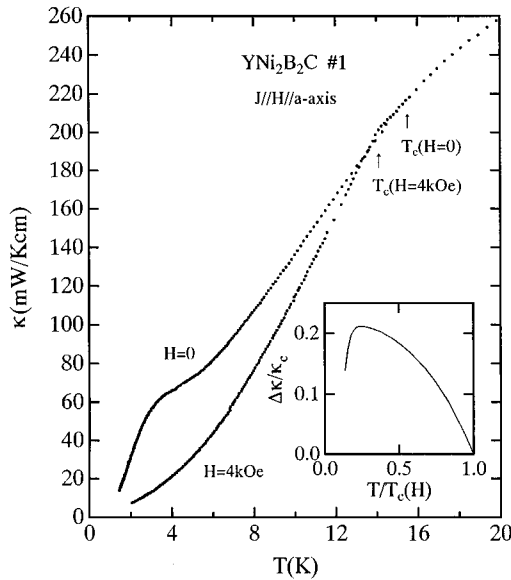


FIG. 2. Temperature dependence of the thermal conductivity with heat current J parallel to the a and c axes of $\text{YNi}_2\text{B}_2\text{C}$ sample 1 under the longitudinal magnetic field. The inset shows the temperature dependence of the difference of the temperature dependence of the thermal conductivities κ_c normalized at $T_c(H)$ between under $H=0$ and $H=4$ kOe.

$\text{YNi}_2\text{B}_2\text{C}$ sample 2 does not show a peak as is seen in sample 1 which may be due to a large residual resistivity in this sample. With the increase of temperature, L/L_0 once becomes smaller than 1, again increases and becomes larger than 1 above ~ 50 K. The fact that $L/L_0 > 1$ at high temperatures above ~ 50 K indicates an increase of the phonon contribution to κ . The fact that $L/L_0 < 1$ in the intermediate-temperature region indicates the existence of the inelastic scattering for electrons. While the effect of the scattering of electrons by long-wavelength acoustic phonons on ρ is small, the thermal conductivity is largely affected through the vertical transition. Different from κ parallel to the a axis, in the case parallel to the c axis, L/L_0 is smaller than 1 in a wide range of temperature. This situation is common to all the samples studied here, which reflects the anisotropic behavior of κ as mentioned above. Further studies are necessary to understand this anisotropy.

Figure 2 shows the temperature dependence of κ parallel to the a axis in the zero magnetic field and under the longitudinal magnetic field of 4 kOe. The thermal conductivity in the zero magnetic field shows the characteristic behavior, i.e., an anomaly at T_c and a pronounced maximum at ~ 4 K as mentioned above. On the other hand, the thermal conductivity under the magnetic field of 4 kOe shows a rapid decrease below T_c ($H=4$ kOe), which is common to conventional superconductors in which heat current is carried mainly by electrons. Figures 3(a) and 3(b) show the longitudinal magnetic-field dependence of the thermal conductivity parallel to the a axis of $\text{YNi}_2\text{B}_2\text{C}$ sample 1. The κ value is largely suppressed by applying a small magnetic field corresponding to H_{c1} and, with further increase of the magnetic field, it is restored to the normal-state value above H_{c2} . The hysteresis is observed below H_{c1} , which is shown in the result at $T=4.3$ K. The similar results are observed also in κ parallel to the a axis under the transverse magnetic field parallel to the c axis. The rapid suppression of the thermal conductivity at $H > H_{c1}$ indicates that heat current is suppressed largely by the existence of vortices. The inset in Fig. 2 shows the temperature dependence of the difference of the thermal conductivities normalized at $T_c(H)$ between under $H=0$ and $H=4$ kOe. This indicates that the contribution from carriers of heat current except electrons to κ increases below T_c in the zero magnetic field because in this temperature region electrons are dominated by the elastic scattering as mentioned above. Considering that this enhancement of κ below T_c is suppressed by introducing vortices and the temperature dependence of κ under $H=4$ kOe is similar to that of the conventional superconductor whose heat current is carried mainly by electrons, it is natural to ascribe the origin of the enhancement of κ below T_c in the zero magnetic field to the increase of the phonon contribution. We simply assume that the total thermal conductivity is expressed as the sum of the phonon and electron contributions, i.e., $\kappa_{\text{tot}} = \kappa_{\text{ph}} + \kappa_e$. The temperature dependence of the difference of the temperature dependence of κ normalized at $T_c(H)$ between under $H=0$ and 4 kOe shown in the inset in Fig. 2 originates from κ_{ph} . κ under $H=4$ kOe mainly originates from κ_e . In the zero magnetic field, the phonon mean free path becomes large below T_c due to the decrease of the number of normal electrons which act as scattering centers of phonons above T_c . This increase of the phonon mean free

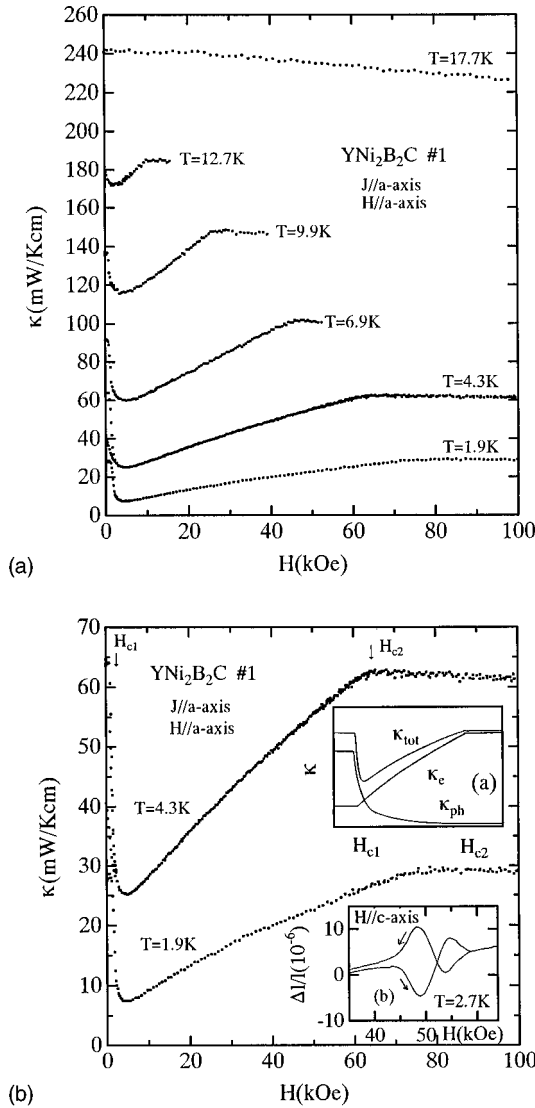


FIG. 3. Magnetic-field dependence of the thermal conductivity with heat current J parallel to the a axis of YNi₂B₂C sample 1 under the longitudinal magnetic field (a) in a temperature region up to 18 K and (b) in a low-temperature region below 4.3 K. H_{c1} and H_{c2} are the lower and upper critical field. Inset (1) shows a schematic picture of κ_{tot} , κ_{ph} , and κ_e . See the text in detail. Inset (2) shows the longitudinal magnetostriction along the c axis in a magnetic field region around H_{c2} .

path causes the additional contribution to κ_e below T_c and this suggests the existence of a large electron-phonon coupling in this material. It is noted that such an enhancement of κ below T_c is not observed in Ba_{1-x}K_xBiO₃ with a relatively high T_c which is considered as the phonon-mediated strong-coupling superconductor.¹²

Next, we discuss the magnetic-field dependence of κ . The phonon thermal conductivity κ_{ph} enhanced below T_c in the zero magnetic field is largely suppressed by vortices introduced at $H > H_{c1}$ because the phonon mean free path decreases as a result that phonons are scattered by vortices. In turn, the electron contribution becomes important with further increase of magnetic field. The schematic picture of the magnetic-field dependence of κ_{ph} and κ_e together with κ_{tot} below T_c is shown in inset (1) of Fig. 3(b). At low tempera-

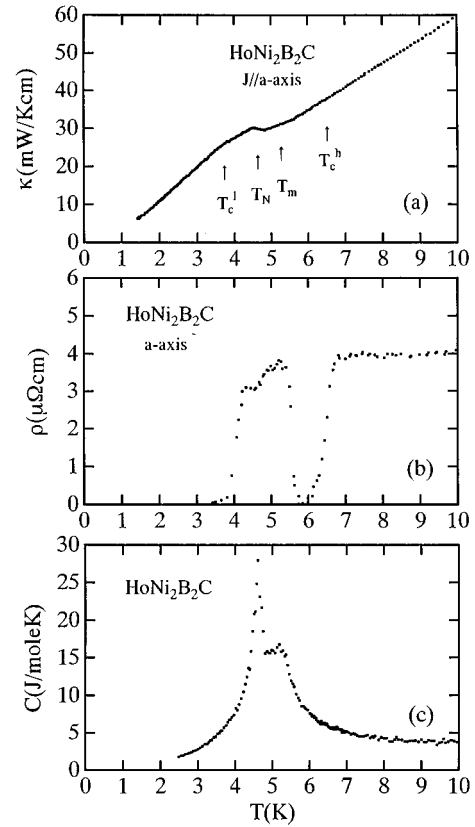


FIG. 4. Temperature dependence of (a) the thermal conductivity, (b) electrical resistivity, and (c) specific heat of HoNi₂B₂C at low temperatures. T_c^h and T_c^l are the higher and lower superconducting transition temperatures, respectively, and T_m and T_N are the incommensurate and commensurate antiferromagnetic transition temperatures, respectively.

tures, the negative curvature of the $d\kappa/dH$ vs H curve is observed, which suggests the possible existence of low-energy excitations in the superconducting state. The temperature dependence of κ under the magnetic field of 4 kOe shows $\sim T^2$ behavior in a wide temperature region below T_c . At present, it is difficult to separate the electron contribution κ_e from κ_{tot} in the superconducting state. Further studies are necessary to understand the magnetic field and temperature dependence of κ below T_c .

The magnetization curve shows the peak effect just below H_{c2} (Ref. 13) which are also observed in UPd₂Al₃ and CeRu₂ (Ref. 14) and has attracted much attention in relation to the possible existence of the Fulde-Ferrell-Larkin-Ovchinnikov state. Inset (2) of Fig. 3(b) shows the longitudinal magnetostriction under the magnetic field parallel to the c axis. This shows the pronounced anomaly in the same magnetic-field region as the peak effect in the magnetization curve is observed, as is observed in UPd₂Al₃ and CeRu₂ (Ref. 14). On the other hand, an anomalous behavior is not observed in κ parallel to the a axis under both longitudinal and transverse magnetic field within our experimental error.

Figures 4(a), 4(b), and 4(c) show the temperature dependence of the thermal conductivity, electrical resistivity, and specific heat of HoNi₂B₂C, respectively. The magnetic properties of this compound were reported in Ref. 15. With the decrease of temperature, the electrical resistivity becomes

nearly zero at the higher superconducting transition temperature $T_c^h \sim 6.6$ K and after recovering to the normal state value at ~ 5.3 K, it becomes zero at the lower superconducting transition temperature $T_c^l \sim 3.6$ K. A small but clear decrease of ρ is observed at 4.6 K. The specific heat shows a small peak at $T_m = 5.3$ K and a large and sharp peak at $T_N = 4.6$ K which correspond to the incommensurate and commensurate antiferromagnetic ordering temperature (Ref. 15), respectively. The large short-range order effect is observed. These results are similar to the reported ones (Refs. 16 and 17) apart from slightly lower transition temperatures in the present sample.¹⁸ At high temperatures, the anisotropic behavior of κ is observed as in $\text{YNi}_2\text{B}_2\text{C}$ and the temperature dependence of L/L_0 is also similar to those of $\text{YNi}_2\text{B}_2\text{C}$. However, low-temperature behavior of κ is different. At higher superconducting transition temperature $T_c^h = 6.6$ K, we could not observe an anomaly in κ . A small but clear increase is observed in κ at T_N . This increase of κ originates from the decrease of ρ accompanying with the decrease of the magnetic scattering of electrons in the antiferromagnetic state. The clear decrease is observed in κ below $T_c^l \sim 3.6$ K.

At present, we do not know whether the heat current is dominated by phonons or electrons in the superconducting state in this compound. In order to clarify it, further studies are necessary at lower temperatures and under the magnetic field.

In conclusion, we have studied the thermal conductivity κ of high-quality $\text{YNi}_2\text{B}_2\text{C}$ and $\text{HoNi}_2\text{B}_2\text{C}$ single crystals. The results of $\text{YNi}_2\text{B}_2\text{C}$ show the followings. The heat current is mainly carried by electrons at low temperatures in the normal state and in the superconducting state, is mainly carried by phonons which may be due to the increase of the phonon mean free path as a result of the decrease of the number of normal electrons below T_c . However, this phonon contribution is easily suppressed by introducing vortices at $H > H_{c1}$ and the electron contribution becomes dominant above H_{c1} . The thermal conductivity of $\text{HoNi}_2\text{B}_2\text{C}$ shows a clear increase just below the Néel temperature 4.6 K and a clear decrease below $T_c^l \sim 3.6$ K.^{17,18}

We are thankful to T. Otomo, H. Miura, S. Tanno, Y. Ishigami, and K. Hosokura of the Tohoku University Cryogenic Center.

¹R. J. Cava *et al.*, Nature (London) **367**, 252 (1994).

²R. Nagarajan *et al.*, Phys. Rev. Lett. **72**, 274 (1994).

³L. F. Mattheiss, Phys. Rev. B **49**, 13 279 (1994).

⁴W. E. Pickett *et al.*, Phys. Rev. Lett. **72**, 3702 (1994).

⁵M. E. Hanson *et al.*, Phys. Rev. B **51**, 674 (1994).

⁶N. M. Hong *et al.*, Physica C **227**, 85 (1994).

⁷S. A. Carter *et al.*, Phys. Rev. B **50**, 4216 (1994).

⁸K. Krishna *et al.*, Phys. Rev. Lett. **75**, 3529 (1995).

⁹H. Takeya *et al.*, Physica C **256**, 220 (1996).

¹⁰T. Terashima *et al.*, Solid State Commun. **96**, 459 (1995).

¹¹M. Sera, S. Kunii, and T. Kasuya, J. Phys. Soc. Jpn. **57**, 13 (1988).

¹²S. D. Peacor *et al.*, Phys. Rev. B **42**, 2684 (1990).

¹³K. Kadowaki *et al.* (unpublished).

¹⁴R. Modler *et al.*, Phys. Rev. Lett. **76**, 1292 (1996).

¹⁵T. E. Grigereit *et al.*, Physica C **248**, 382 (1995).

¹⁶M. S. Lin *et al.*, Phys. Rev. B **52**, 1181 (1995).

¹⁷P. C. Canfield *et al.*, Physica C **230**, 397 (1994).

¹⁸H. Takeya *et al.* (unpublished).